

## Atomic dynamics in liquid alkali metals at the melting point

Kirit N. Lad\* and Arun Pratap

Condensed Matter Physics Laboratory, Applied Physics Department, Faculty of Technology & Engineering, M. S. University of Baroda, Vadodara-390001, Gujarat, India

(Received 5 May 2005; revised manuscript received 1 December 2005; published 27 February 2006)

The atomic dynamics in liquid alkali metals at the melting point has been studied with the help of an equation of motion in terms of the velocity autocorrelation function. An atom is considered to be moving in a mean-time-dependent field, in a series of steps much smaller than the average interatomic spacing (small-step diffusion approximation). The theoretical formulation presented here is a special case of our generalized formulation for simple monatomic liquids [Phys. Rev. E. **70**, 51201 (2004)]. It gives a good account of the single-particle motion in liquid Li, Na, K, Rb, and Cs. The calculated self-diffusion coefficients are found to be in excellent agreement with the experiments. The formulation is also used to investigate the collective excitations arising due to density fluctuations. The dispersion curves for the collective excitations for Li, Na, and K show a decent overall agreement with the inelastic neutron scattering and inelastic x-ray scattering results. The effect of quantum-mechanical correction has been observed for Li, Na, and K. It suggests a significant improvement over the classical results. Since the applicability of the small-step diffusion approximation is limited to weak electron-ion coupling at high electron densities, the present formulation gives satisfactory dispersion curves for Rb and Cs in a small intermediate  $q$  range. It has been observed that an abrupt change in the dynamical properties occurs at the position of potassium in accordance with the change in atomic number density.

DOI: [10.1103/PhysRevB.73.054204](https://doi.org/10.1103/PhysRevB.73.054204)

PACS number(s): 61.25.Mv, 66.30.Fq, 05.40.Jc

### I. INTRODUCTION

At the microscopic scale, the individual atomic motion in dense liquids is quite different from simple diffusion and is often described qualitatively as a superposition of diffusive and oscillatory motions. It is now established from the experimental and theoretical investigations<sup>1-5</sup> that the dynamical behavior of a simple liquid is associated with at least two time scales corresponding to “fast” ( $\beta$ ) and “slow” ( $\alpha$ ) relaxation processes. The short-time scale ( $\tau_\beta$ ) for  $\beta$ -relaxation process corresponds to the vibratory motion of an atom about a quasifixed position, being temporarily “caged” by neighboring atoms. The long-time scale ( $\tau_\alpha$ ) for  $\alpha$ -relaxation process corresponds to the translational motion of atoms in a liquid, due to the breaking of the “cages” by cooperative rearrangements of the neighboring atoms.

The phenomenological understanding of the process of self-diffusion in liquids relies on the concepts of Brownian motion wherein the classical Langevin equation describes the motion of an atom in an environment in statistical equilibrium. The classical Langevin equation involves a single relaxation time ( $\beta$ ) known as the friction coefficient related to the systematic part of the interatomic force field. Further, it is valid when the mass of the diffusing atom is much larger than the surrounding atoms, and fails when the mass of the diffusing atoms is comparable or same as the mass of the surrounding atoms. Hence, for dense liquids such as liquid alkali metals the Langevin equation must be modified so that it can account for the two relaxation processes related to the aforementioned time scales of atomic motion. A successful attempt in this direction was made by Glass and Rice<sup>6</sup> (GR) to describe the single particle motion in monatomic classical liquids such as liquid argon. Assuming a Brownian particle

diffusing in a mean-time-dependent field, they have modified the classical Langevin equation by adding another systematic force term representing the time-dependent force field. (For details see Ref. 6.) Subsequently, they have derived an equation of motion in terms of velocity autocorrelation function (VACF)  $\psi(t)$  as

$$\frac{d^2\psi}{dt^2} + (\alpha + \beta)\frac{d\psi}{dt} + (\omega^2 e^{-\alpha t} + \alpha\beta)\psi = 0. \quad (1)$$

It explicitly involves two relaxation rates  $\alpha$  and  $\beta$ . Where  $\alpha^{-1}$  corresponds to the time for which an atom remains in the same local environment before diffusing away, i.e., the time an atom spends in its nearest neighbor cage before diffusing out as a result of breaking of the cage due to the cooperative or structural rearrangements. The friction constant  $\beta$  represents the damping of the oscillatory motion of atoms inside the cage on account of “backscattering” from the wall of the cage. Evidently, the relaxation rate  $\beta$  will be larger than  $\alpha$ . The exact solution of Eq. (1) can be obtained, given *a priori* knowledge of  $\alpha$  and  $\beta$ . However, due to difficulty in the accurate calculation of  $\alpha$ , a simplified solution of Eq. (1) is obtained by GR assuming the two relaxation rates to be equal. In our recent work<sup>7</sup> (referred to as paper I now onwards), we have shown that this assumption ( $\alpha = \beta$ ) holds good for insulating fluids such as argon at 85 K whereas it is not true for high density liquids such as liquid alkali metals. In paper I, we provided a generalized solution of Eq. (1) subject to the condition  $\alpha \neq \beta$ . Though the generalized solution gives promising results for VACF in pure liquid alkali metals and its alloys, it depends on the knowledge of diffusion coefficient ( $D$ ) which is an essential input parameter. However, if we know the ratio ( $\beta/\alpha$ ) we can do away with

the parameter  $D$ . In paper I, we observed that for liquid Li and Na at the melting point,  $\beta$  is three times as large as  $\alpha$ . This result, and the unique universal behavior in their properties<sup>8,9</sup> displayed by the liquid alkali metals, prompted us to assume  $\beta=3\alpha$  to be universal among liquid alkali metals. This assumption greatly simplifies the evaluation of VACF in liquid alkali metals at the melting point. Further, we also assume that the diffusion in dense liquids proceeds by a series of displacements each small compared to the interatomic spacing.<sup>10</sup> According to this assumption, also known as the small-step diffusion approximation (SSDA), the gradient of the pair interaction potential between molecules at time  $(t+s)$  can be expanded in a Taylor series about the gradient at time  $t$  and terms higher than the second may be neglected. The expansion is considered to be valid for soft collisions<sup>10</sup> which is exactly the case for liquid alkali metals showing a much softer repulsive core interaction compared to the liquefied inert gases.<sup>11</sup> These assumptions facilitate the determination of VACF in liquid alkali metals (Li, Na, K, Rb, Cs) with the help of the generalized solution of Eq. (1), the effective pair potentials and the pair correlation function. The VACF can easily be integrated to obtain the diffusion coefficient. It can also be used to study the mean square displacement, the dynamical structure factor  $S(q, \omega)$  and the dispersion of collective excitations in liquid alkali metals.

The paper is organized as follows. Section II gives a brief description of the second-order perturbation theory used to obtain the effective pair potentials in the liquid alkali metals at the melting point. The formulas and equations necessary to calculate the VACF, derived from our generalized approach in paper I, are narrated in Sec. III. Section IV deals with our results and discussion for the VACF, diffusion coefficient, mean square displacement and dispersion of collective excitations. Finally, concluding remarks of the present study are given Sec. V.

## II. INTERATOMIC PAIR POTENTIAL

The most popular route to obtain the interatomic pair potentials in the liquid metals is to use pseudopotentials in second-order perturbation theory. Accordingly, the effective pair potential can be given by

$$V(r) = \frac{(Ze)^2}{r} - \frac{2(Ze)^2}{\pi} \int_0^\infty F_N(q) \frac{\sin qr}{qr} dq. \quad (2)$$

The first term on the right-hand side (RHS) of Eq. (2) represents the Coulombic ion-ion interaction which is repulsive in nature whereas the second term gives attractive force arising due the presence of conduction electrons.  $F_N(q)$  is the wave-number-energy characteristic and is given by

$$F_N(q) = \frac{\Omega^2 q^4}{16\pi^2 z^2 e^4} \left(1 - \frac{1}{\epsilon(q)}\right) \left(\frac{1}{1 - G(q)}\right) w^2(q), \quad (3)$$

where  $w(q)$  is the form factor and is the Fourier transform of the pseudopotential. The evanescent core pseudopotential proposed by Fiolhais *et al.*<sup>12</sup> has been widely utilized to study the dynamical properties of liquid alkali metals.<sup>13,14</sup> In the present work, we have also used the evanescent core

TABLE I. Parameters of the evanescent core potential in the individual ( $I$ ) form (Ref. 12).

Metal	$A$	$R$ (Å)
Li	4.113	0.181
Na	3.499	0.261
K	3.321	0.361
Rb	3.197	0.402
Cs	3.138	0.449

pseudopotential where the form factor is given by

$$w(q) = 4\pi ZR^2 \frac{N}{V} \left[ -\frac{1}{(qR)^2} + \frac{1}{(qR)^2 + a^2} + \frac{2ab}{[(qR)^2 + a^2]^2} + \frac{2A}{[(qR)^2 + 1]^2} \right]. \quad (4)$$

In order to avoid confusion, the parameters  $\alpha$  and  $\beta$  in the formalism given by Fiolhais *et al.*<sup>12</sup> have been replaced by  $a$  and  $b$ , respectively.  $R$  is the core decay length.  $A$  and  $b$  are expressed in terms of  $a$  as

$$A = \frac{a^2}{2} - ab, \quad (5)$$

$$b = \frac{a^3 - 2a}{4(a^2 - 1)}. \quad (6)$$

In Ref. 12, two versions of the evanescent core pseudopotential have been given with universal ( $U$ ) and individual ( $I$ ) choices for the parameters  $a$  and  $R$ . We have obtained the results for the individual version of the potential and the values for the parameters are listed in Table I. The terms  $\epsilon(q)$  and  $G(q)$  in Eq. (3) are the dielectric screening function and the local-field correction, respectively.  $G(q)$  takes into account the electron-ion coupling due to the exchange-correlation (XC) effects between conduction electrons. A relevant parameter giving the measure of the electron-ion coupling is defined as the Coulomb coupling constant  $r_s = (3/4\pi\rho)^{1/3} 1/a_0$ , where  $\rho$  is the atomic number density and  $a_0$  is the Bohr radius. A variety of expressions for  $G(q)$  are available in the literature and is an important aspect of pseudopotential formalism. In the present work, we have used the expression proposed by Ichimaru and Utsumi<sup>15</sup> (IU) which deals with the electron densities corresponding to  $0 \leq r_s \leq 15$ . Thus, applicability of IU expression extends much beyond the random phase approximation (RPA) limit ( $r_s \ll 1$  at high electron densities). The formulation used here for the description of atomic motion employs the SSDA which corresponds to the weak electron-ion coupling. Hence, the local-field correction  $G(q)$  is of significant importance in understanding the atomic dynamics in liquid alkali metals.

## III. MATHEMATICAL FORMULATION

In paper I, we have given a detailed solution of the equation of motion (1) to obtain the VACF in terms of  $n$ th order

Bessel functions of the first and second kind. The order ( $n$ ) is defined as  $n = \beta/\alpha - 1$ . Although it is difficult to evaluate  $\alpha$  accurately, one can estimate it by the memory function approach<sup>16</sup> where the choice of a proper kernel  $K(t)$  representing the memory function is important. The approximate memory function representation by Berne *et al.*<sup>17</sup> enables the evaluation of  $\alpha$  in terms of the mean-square force  $\langle \nabla^2 V \rangle$ , mass  $M$  and friction constant  $\beta$ . As mentioned earlier, we will assume in the following  $\beta = 3\alpha$ . This is in concurrence with the observation made by Balucani *et al.*<sup>18</sup> about the VACF memory function  $[K(t)]$  describing the single-particle dynamics in simple liquids. The memory function is split as  $K(t) = K_B(t) + K_R(t)$ . Where  $K_B(t)$  accounts for the initial fast decay due to rapid “binary” collisional events characterized by a time  $\tau_B$ , and  $K_R(t)$  corresponds to the long-lasting “recollisional” effects that are basically due to the sluggishness of structural relaxation. It has been pointed out that at the short-time scale,  $K(t)$  is almost governed by the binary portion  $K_B(t)$  which, however, becomes negligible after a time of the order of  $3\tau_B$  and henceforth; the dynamics of the memory function is entirely determined by the long-lasting contribution  $K_R(t)$ . Therefore, in such a situation, the order  $n$  turns out to be equal to 2 and the problem of determining the VACF reduces to a special case ( $n=2$ ) of our generalized solution of Eq. (1) given in paper I. Then, the equations and formulas necessary for the present calculations can be derived merely substituting  $n=2$ .

Substituting

$$u = 6\gamma e^{-(1/6)\beta t} \quad (7)$$

with  $\gamma = \omega/\beta$ , the solution of Eq. (1) can be given by

$$\psi(t) = e^{-(2/3)\beta t} v(u), \quad (8)$$

where  $v(u)$  is the solution of the Bessel equation

$$u^2 v'' + uv' + v[u^2 - 2^2] = 0. \quad (9)$$

Solving Eq. (9), Eq. (8) can be written in terms of Bessel functions of first and second kind as

$$\psi(t) = e^{-(2/3)\beta t} [c_1 J_2(u) + c_2 Y_2(u)], \quad (10)$$

where  $c_1$  and  $c_2$  can be given by

$$c_1 = -\frac{Y_2(6\gamma) - \gamma Y_3(6\gamma)}{\gamma [J_2(6\gamma)Y_3(6\gamma) - J_3(6\gamma)Y_2(6\gamma)]}, \quad (11)$$

$$c_2 = \frac{J_2(6\gamma) - \gamma J_3(6\gamma)}{\gamma [J_2(6\gamma)Y_3(6\gamma) - J_3(6\gamma)Y_2(6\gamma)]}. \quad (12)$$

Equations (7)–(12) can be easily derived by substituting  $n=2$  in Eqs. (13)–(18) of paper I. The equations necessary for dealing with the parameter  $\omega$  in Eq. (1) are obtained using Eqs. (21) and (24) of paper I and are given by

$$\omega^2 \left[ 1 + \frac{1}{3\gamma^2} \right] = \frac{\langle \nabla^2 V \rangle}{3M}, \quad (13)$$

$$\frac{\beta}{\omega^2} \left[ 1 + \frac{2c_2}{27\gamma^2\pi} \right] = \frac{MD}{k_B T}, \quad (14)$$

where

$$\langle \nabla^2 V \rangle = 4\pi\rho \int_0^\infty dr r^2 g(r) \left( \frac{\partial^2 V}{\partial r^2} + \frac{2}{r} \frac{\partial V}{\partial r} \right), \quad (15)$$

$g(r)$  being the pair distribution function and  $\rho$ , the atomic number density.  $(\partial V/\partial r)$  and  $(\partial^2 V/\partial r^2)$  are the first and second order derivatives of the interatomic pair potential  $V(r)$ .

It should be noticed that determination of  $\gamma$  is necessary for the above formulation to be useful. The procedure given by GR to obtain  $\gamma$  involves the static-harmonic-well (SHW) model.<sup>19</sup> Using the definitions of  $\beta_0$  and  $\omega_0$  given in the SHW model, we can express  $\beta$  and  $\omega$  in terms of  $\gamma$  and  $\omega_0$ . The SHW model, in analogy with the theory of solids, describes the Brownian motion of a harmonically bound particle in a square well (or a cage) formed by the nearest-neighbor atoms. The seemingly abrupt introduction of the SHW model and the concept of harmonically bound particle may arouse suspicion about its application in a model where a Brownian particle is assumed to diffuse in a mean-time-dependent force field. GR, in their formulation, use a spherically symmetric harmonic force field which decays exponentially as time increases whereas in SHW model the force is independent of time and depends on position only. Thus, the square-well, which is considered to be static in SHW model, does not relax for a very long time ( $\tau_\alpha \rightarrow \infty$  or  $\alpha \rightarrow 0$ ) giving rise to the persistent oscillations of the atom inside the well. In case of GR model, however, the well is considered to be quastatic, i.e., the well is static up to the time the nearest-neighbor cage relaxes due to the cooperative motion of atoms in the liquid. We have already noted that  $\tau_B < \tau_\alpha$ . So, the SHW can be conveniently used to calculate  $\omega_0$  in the GR model. Hence, for  $\alpha=0$ , Eq. (1) reduces to the equation of motion for a harmonic oscillator [Eq. (25) of paper I]<sup>20</sup> with the terms  $\beta$ ,  $\omega$  replaced by  $\beta_0$ ,  $\omega_0$  respectively, and defined in Eqs. (28), (29) of paper I. Using these definitions in Eq. (14) we obtain

$$\omega = \sqrt{3}\omega_0 \gamma [1 + 3\gamma^2]^{-1/2}, \quad (16)$$

$$\beta = \sqrt{3}\omega_0 [1 + 3\gamma^2]^{-1/2}, \quad (17)$$

where  $\gamma$  is determined by the solving the following equation which is obtained by substituting Eqs. (16) and (17) in Eq. (14),

$$\left( 1 + \frac{2c_2}{27\gamma^2\pi} \right) = \sqrt{3} \frac{\beta_0}{\omega_0} \gamma^2 [1 + 3\gamma^2]^{-1/2}. \quad (18)$$

Thus, in order to solve Eq. (18) we should know  $\beta_0/\omega_0$ .  $\beta_0$  can be determined from the knowledge of  $D$ . However, if we take  $\beta_0 = \omega_0$ , we can dispose of  $D$ . It is indeed the condition if we assume small-step diffusion. Assuming small-step diffusion in dense fluids, the friction coefficient ( $\beta_0$ ) can be expressed in terms of the intermolecular potential and the local equilibrium pair correlation function as<sup>10</sup>

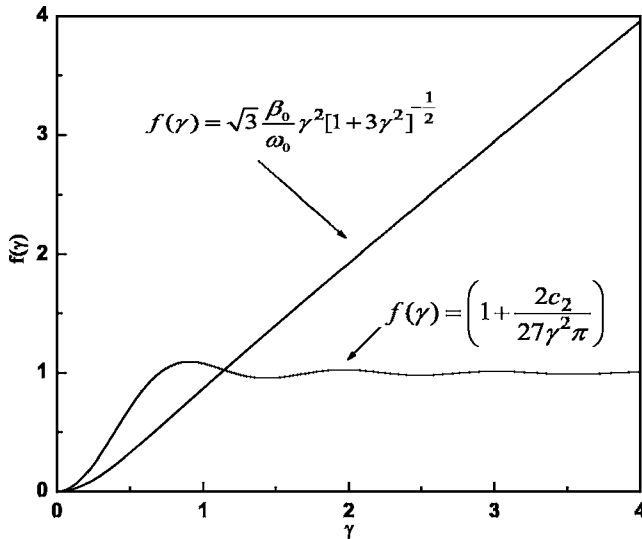


FIG. 1. Two sides of Eq. (18) plotted as a function of  $\gamma$  for the case  $\beta_0 = \omega_0$ .

$$\beta_0^2 = \frac{4\pi\rho}{3M} \int dr r^2 g(r) \nabla^2 V(r). \quad (19)$$

Then, the definition of  $\omega_0$  [Eq. (28) of paper I] alongwith Eq. (15) gives  $\beta_0 = \omega_0$ . In order to understand the physical implication of this condition, consider the motion of an arbitrary atom inside its nearest-neighbor cage. The atom moves in a series of displacements ( $\Delta r$ ) which are much smaller than the interatomic distance. The motion of the atom is influenced by the damping force due to its interaction with the cage atoms. Note that  $\beta_0$  is a relaxation time associated with the damping force and  $\omega_0$  is related to the time period of oscillation of an atom inside the cage on account of backscattering from the cage wall. Hence,  $\beta_0 = \omega_0$  implies that the time for the relaxation of the damping force is equal to the time taken by the atom moving in a cage to complete oscillation around a quasifixed position. This picture of atomic motion inside a nearest-neighbor cage is in line with the itinerant oscillator model<sup>21</sup> and is just an approximate qualitative view of what could be the atomic motion at the time scale in the consideration. However, it does suggest that there would be at least two collisions of a moving atom with the cage wall before the relaxation of the damping force. This inference becomes relevant in light of the results reported by Harris and Rice.<sup>22</sup> For the case of the dense rigid sphere fluid, they have calculated the longest relaxation time for the return to equilibrium of a distribution perturbed in momentum space but always at equilibrium in configuration space. In the gas phase the time required corresponded to approximately four collisions. However, at liquid densities, the time required corresponded to only one collision. For  $\beta_0 = \omega_0$ , plotting the two sides of Eq. (18) as a function of  $\gamma$  (Fig. 1), we can see that there is one root and we find  $\gamma = 1.1475$ ,  $c_1 = -3.3589$ ,  $c_2 = 1.3974$ . Thus, the above formulation for  $n=2$  and  $\beta_0 = \omega_0$ , can be used to obtain the VACF for the liquid alkali metals at the melting point. The so-obtained VACF can be utilized to determine the self-diffusion coefficient ( $D$ ) and the mean-square displacement ( $\langle r^2(t) \rangle$ ).

Present description of atomic motion is also analogous to the interpolation model<sup>23</sup> where the atoms are considered to be moving in relaxing cages. An atom behaves as an oscillator with characteristic frequency  $\omega_0$  during short times and as a diffusing particle with friction coefficient  $\beta_0$  at long times. Using the interpolation model, the coherent scattering function (also known as dynamic structure factor)  $S(q, \omega)$  can be obtained from the knowledge of the mean-square displacement and the static structure factor  $S(q)$  as

$$S(q, \omega) = \frac{S(q)}{\pi} \int_0^\infty dt \cos \omega t \exp[-q^2 \langle r^2(t) \rangle / 6S(q)]. \quad (20)$$

Equation (20) is obtained using the following approximations.

(i) Convolution approximation (CA) by Vineyard<sup>24</sup> given as  $S(q, \omega) \approx S(q)S_{\text{self}}(q, \omega)$ .

(ii) Skold conjecture,<sup>25</sup> which is based on the fact that the CA does not reproduce the second moment as calculated by DeGennes.<sup>26</sup> Therefore, the CA is modified to  $S(q, \omega) \approx S(q)S_{\text{self}}\{q[S(q)]^{-1/2}, \omega\}$ . An analogous result has also been reported by Venkataraman *et al.*<sup>27</sup> This procedure of the modification of CA has been referred to as the effective-mass approximation (EMA) by Desai and Yip.<sup>23</sup>

(iii) Gaussian approximation on  $S_{\text{self}}(q, \omega)$  which is well described by Rahman *et al.*<sup>28</sup> It is argued that it holds exactly in the special cases of a harmonic solid, ideal gas and a system for which the motion of atom is governed by Langevin's equation.

Though the EMA gives reasonable results over practically entire range of  $(q, \omega)$ ,<sup>23</sup> the validity of GA must be ensured for the calculation of  $S(q, \omega)$ . This would also be of interest in light of the recent investigations by Colognesi *et al.*<sup>29</sup> reporting the breakdown of the GA in the semiquantum liquids. The quantized character of the energy transfers at a microscopic level leads to a natural unbalance of the spectral properties of a system, depending whether energy gains or losses are considered. The classical treatment of these features is approximately valid only for frequencies  $\omega$  such that  $\hbar\omega/k_B T \ll 1$ . This factor, being nearly 0.7, 0.3, and 0.2 for Li (463 K), Na (378 K), and K (343 K), respectively, at  $\omega_0$  (see Table II), is obviously not negligible compared to 1. Hence, we shall see that the relevant quantum effects provide significant improvement in the dispersion curves [Sec. IV D]. The GA is exact both in the long time diffusive regime (hydrodynamic limit,  $q \rightarrow 0$ ) and the short time free-particle limit (short-wavelength, large  $q$ ).<sup>1</sup> However, it is noteworthy here that in accordance with an analogous model given by Venkataraman *et al.*,<sup>27</sup> Eq. (20) would not be valid at very large times and would not tend to the hydrodynamic limit. In the intermediate  $q$  range [where  $q$  is near the position  $q_0$  of the main peak of  $S(q)$ ], discrepancies arise due to the presence of non-Gaussian terms.<sup>1,18</sup> For the satisfactory understanding of the single-particle dynamics these “non-Gaussian” corrections should be investigated. But, the calculation of the non-Gaussian corrections is a rather involved process and for the case of liquid argon they are



TABLE II. Input parameters for the velocity autocorrelation function.

Metal	$T$ (K)	$M$ ( $10^{-23}$ g)	$\rho$ ( $10^{24}$ cm $^{-3}$ )	$\alpha$ ( $10^{13}$ s $^{-1}$ )	$\beta=3\alpha$ ( $10^{13}$ s $^{-1}$ )	$\langle \nabla^2 V \rangle$ ( $10^5$ erg cm $^{-2}$ )	$\omega_0 = \langle \langle \nabla^2 V \rangle / 3M \rangle^{1/2}$ ( $10^{12}$ s $^{-1}$ )
Li	463	1.152	0.0444	2.473	7.419	0.634	42.8
Na	378	3.816	0.0242	0.932	2.795	0.298	16.1
K	343	6.491	0.0128	0.543	1.628	0.172	9.4
Rb	313	14.188	0.0104	0.323	0.968	0.133	5.6
Cs	303	22.061	0.0083	0.250	0.749	0.124	4.3

shown to be relatively small.<sup>30</sup> In the case of liquid Li near melting, the discrepancies introduced by GA in  $S(q, \omega)$  are shown to be rather small and restricted to the frequency region close to  $\omega=0$ .<sup>31</sup> Thus, notwithstanding the importance of non-Gaussian correction, GA can give a decent overall description of single-particle dynamics with a realistic model for the mean-square displacement.  $S(q, \omega)$  is directly related to the spectrum of the longitudinal current fluctuations. The maximum  $[\omega_m(q)]$  of the longitudinal current-current correlation spectra

$$J_L(q, \omega) = \frac{\omega^2}{q^2} S(q, \omega) \quad (21)$$

gives the information about the dispersion of collective excitations in the liquid alkali metals.

## IV. RESULTS AND DISCUSSION

### A. Interatomic pair potentials

The interatomic pair potentials for the liquid alkali metals at their melting point are shown in Fig. 2. It exhibits the characteristic features of the interatomic potential in the liquid metals: (i) the relatively soft repulsive core and (ii) the oscillatory tail due to the attractive forces which arise from the presence of the conduction electrons. In order to check the universality of the behavior of alkali metals, the poten-

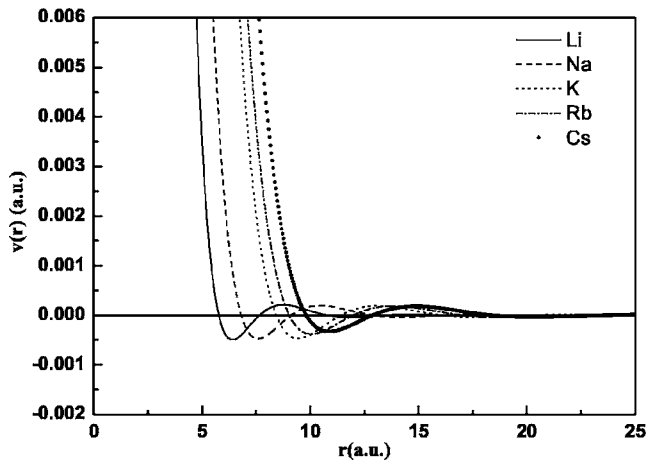


FIG. 2. Interatomic pair potentials for the liquid alkali metals: Li (—), Na (---), K (⋯), Rb (-.-), Cs (⋯).

tials can be shown to fall on a single curve (Fig. 3) in terms of the reduced units. It is noteworthy that K, Rb, and Cs are described by a similar repulsive potential which differs from that of Li and Na (Fig. 2). Since the repulsive potential is directly related to the atomic number density, the trend in the interatomic pair potential is in accordance with the trend in the atomic number density of the alkali metals at the melting point (Fig. 4).<sup>32</sup> An abrupt change in the number density occurs at K. The repulsive potential plays a significant role in the motion of atoms at short-time scale (of the order of picosecond). Consequently, similar trend has also been observed for VACF.

### B. Velocity autocorrelation function

Figure 5 shows the VACF for the liquid alkali metals at their melting point obtained from Eq. (10). The essential input parameters are summarized in Table II. The VACFs for the liquid alkali metals exhibit the “backscattering region”—a negative region—corresponding to the reversal of velocity of an atom after collision with the wall of the nearest-neighbor cage. However, the long-time oscillations, the characteristic of VACF in liquid metals are absent. The absence of the long-time oscillations in the VACF can be attributed to the small-step diffusion approximation which is considered to be valid for soft collisions.<sup>10</sup> The soft collision

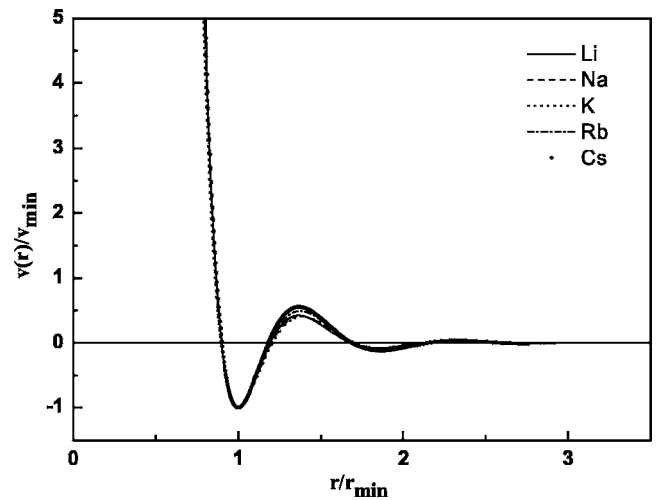


FIG. 3. Interatomic pair potentials for the liquid alkali metals in terms of reduced units. Legends are the same as in Fig. 2.

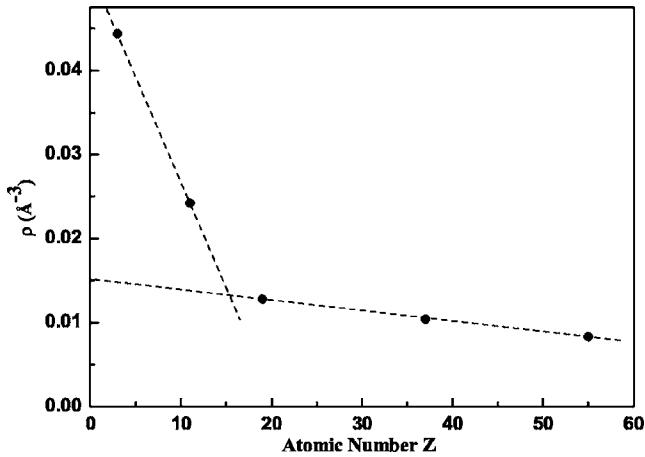


FIG. 4. Atomic number density ( $\rho$ ) of alkali metals at the melting point versus the atomic number  $Z$ . The dashed line shows the trends in the change in the number density.

picture is reasonably correct for the liquid alkali metals which possess much softer repulsive core compared to the liquefied inert gases.<sup>11</sup> Further, the attractive forces, arising due to the presence of conduction electrons in liquid metals, increase the cohesiveness of the cage formed by the nearest neighbors.<sup>33</sup> Due to strong cohesion, when an atom collides with a neighbor, the momentum transfer is with a significant part of the nearest-neighbor cage and the atom rebounds from the greater mass.<sup>34</sup> Hence, as a result of soft collision and the strong cohesion, the decay of the VACF in liquid alkali metals is highly damped as observed from the present results. It is evident from Figs. 2 and 5 that the repulsive core has significant effect on the atomic motion at short time scales. The average backscattering time is determined primarily by the softness of the interatomic repulsion.<sup>35</sup> As the softness of the repulsive potential increases, the average backscattering time increases regularly. The backscattering time can be identified with the initial decay time ( $\tau_D$ ) for the

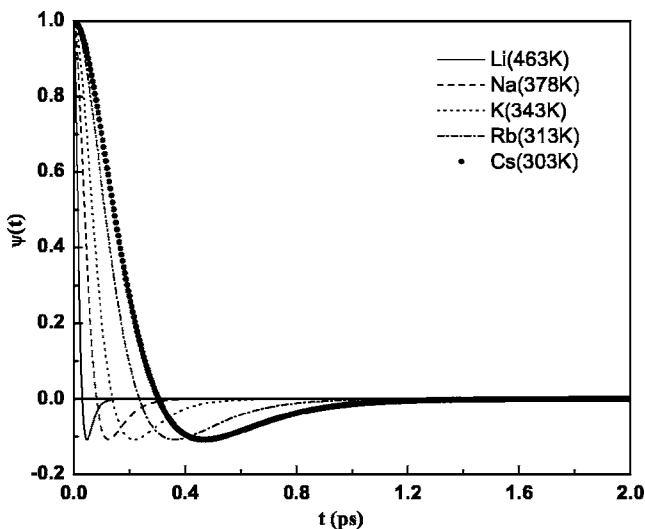


FIG. 5. Velocity autocorrelation function for the liquid alkali metals at the melting point obtained using Eq. (10). Legends are the same as in Fig. 2.

TABLE III. Diffusion coefficients (in units  $10^{-5} \text{ cm}^2 \text{ S}^{-1}$ ) for liquid alkali metals at melting point.

Metal	$T$ (K)	$D_{\text{cal}}$	$D_{\text{MSD}}$	$D_{\text{expt}}$
Li	463	5.82	5.82	6.1–6.8
Na	378	3.81	3.81	4.06–4.35
K	343	3.49	3.49	3.52–3.72
Rb	313	2.45	2.46	2.60
Cs	303	1.97	2.00	2.16

memory function of the VACF. At  $\tau_D$ , the velocity of the diffusing particle is reversed on account of backscattering. Gonzalez *et al.*<sup>31</sup> and Dalgic *et al.*<sup>13</sup> have reported  $\tau_D$ , in case of Li, to be 0.034 ps which in the present study is found to be 0.031 ps. Further,  $\tau_D$  obtained for Rb (0.235 ps) and Cs (0.304 ps) is also in close agreement with values given by Dalgic *et al.*<sup>13</sup> for Rb and Cs to be equal to 0.234 and 0.324 ps, respectively. The softness of the interatomic repulsion also governs the coherence of the backscattering events (or correlation of the atomic collisions) which eventually influences the negative region of VACF. For a hard sphere fluid, the backscattering events occur less coherently and hence show less inclination to have negative region.<sup>36</sup> Thus, the liquids with soft interatomic repulsion are expected to produce pronounced negative regions. Present results for the liquid alkali metals provide a testimony to this reasoning. The increase in the softness of the repulsive core from Li to Cs results into pronounced (in time) negative regions in the VACF (Fig. 5). Since the self-diffusion coefficient ( $D$ ) is the time integral of the VACF, the backscattering region is very important for the determination of  $D$  in liquids. The absence of negative region would lead to a very high value of  $D$ . The calculated values of  $D$  for the liquid alkali metals at their melting point are given in Table III. It can be seen that the values obtained from the present calculations are in close agreement with the experimental results. The maximum deviation of the calculated  $D$  from the experimental values is upto 14% (for Li).

The universal behavior of effective pair potential in liquid alkali metals is already demonstrated in Fig. 3. In order to check whether a similar behavior is displayed by the liquid alkali metals in case of VACF, we have plotted VACFs of these metals in reduced units [ $\psi(t)/\psi_{\text{min}} \rightarrow t/t_{\text{min}}$ ] as shown in Fig. 6. All the VACFs fall on a single curve and they are indistinguishable from each other. This result is in agreement with molecular dynamics reports.<sup>8</sup> It is yet another indication that our simple formulation in the present work could successfully describe the self dynamical behavior of the liquid alkali metals at short time scales.

### C. Mean square displacement

The mean square displacements for the liquid alkali metals, obtained using VACFs, are shown in Fig. 7. It depicts, (i) the short-time single-particle motion where  $\langle r^2(t) \rangle_{t \rightarrow 0} \propto t^2$  and (ii) the long-time diffusive motion where  $\langle r^2(t) \rangle_{t \rightarrow \infty} \propto 6Dt$ . The slope of the linear diffusive part gives the diffusion co-

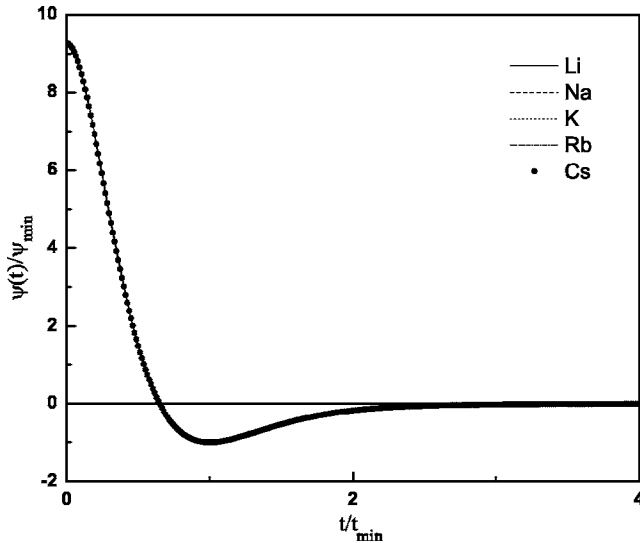


FIG. 6. Velocity autocorrelation function for the liquid alkali metals at the melting point. Legends are the same as in Fig. 2. All the VACFs fall on a single curve and are indistinguishable.

efficient. The values of  $D$  for the liquid alkali metals evaluated from the linear part of the mean square displacement are given in Table III. The results are consistent with those obtained from VACF and the experiments. The inset in the Fig. 7 shows that the time, for which single-particle behavior persists, is  $\sim 0.2$  ps for K, Rb, and Cs while it is  $\sim 0.03$  ps for Li and Na. The longer-time of single-particle motion in K, Rb, and Cs is attributed to the softer repulsive core in the interatomic potential. The soft repulsive core supports the long-lasting density fluctuations in the liquid alkali metals.

#### D. Dispersion of collective excitations

The maxima of longitudinal current-current correlation spectra [Eq. (21)] at different  $q$  give the dispersion curves

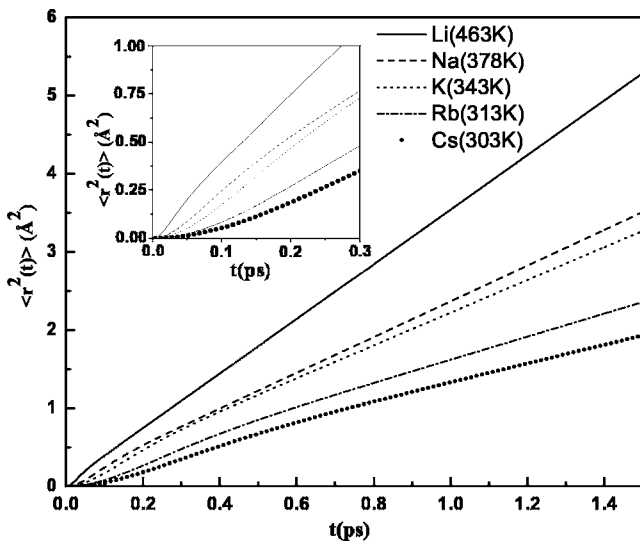


FIG. 7. Mean square displacement for the liquid alkali metals at the melting point. Legends are the same as in Fig. 2. Inset in the figure shows the  $t^2$  dependence of mean square displacement for single-particle motion at short times.

$[\omega_m(q) \rightarrow q]$  for the collective excitations. The dispersion curves for the liquid alkali metals (Li, Na, K, Rb, and Cs) are given in Figs. 8(a)–8(e). Present results are compared with the results of the inelastic x-ray scattering (IXS) and/or inelastic neutron scattering (INS) experiments. For Li and Na, the dispersion curves are in good agreement with the experiments and exhibits the characteristic features: (i) the dispersion is almost linear at low  $q$ -typical of a sound wave. The so-called positive dispersion, a fingerprint of the relaxation dynamics of disordered systems-either liquid or glassy-reflects the host of mechanisms driving such dynamics and their time scale.<sup>37</sup> (ii) Between the low- $q$  region and the high- $q$  limit,  $\omega_m(q)$  exhibits oscillations which are in phase with the structural correlations as observed in  $S(q)$ . For example, the position of the first maximum is at about  $q = q_0/2$ ,  $q_0$  being the position of the first peak in  $S(q)$ .

The definitions of  $S(q, \omega)$  [Eq. (20)] and  $J_L(q, \omega)$  [Eq. (21)] used in the present calculations is valid for classical systems. However, the quantum mechanical corrections are shown to be of significant importance in case of Li. As reported by Scopigno *et al.*,<sup>37,38</sup> the main effect of quantum-mechanical corrections stems from the well-known inequality of the positive and negative frequency parts of the spectra, connected by the detailed balance factor  $\exp(\hbar\omega/k_B T)$ . Another source of nonclassical behavior is associated with a finite value of the De Broglie wavelength  $\Lambda = (2\pi\hbar^2/mk_B T)^{1/2}$  which being very small (for Li,  $\Lambda$  being only 0.11 times the average interatomic distance) can be safely neglected. In order to account for the effect of the detailed balance factor, the  $S_Q(q, \omega)$  is given as

$$S_Q(q, \omega) = \frac{\hbar\omega/k_B T}{1 - e^{-\hbar\omega/k_B T}} S_{Cl}(q, \omega), \quad (22)$$

where the subscript Q and Cl correspond to quantum and classical cases, respectively. Thus, for  $\hbar\omega/k_B T \ll 1$ ,  $S_Q(q, \omega) \approx S_{Cl}(q, \omega)$ . However, as noted earlier, this is not the case for Li, Na, and K; and significant effect of the quantum corrections should be observed. As a result of quantum corrections, Figs. 8(a)–8(c) exhibit a noteworthy improvement in the dispersion curves of Li, Na, and K, respectively. The quantum corrections are observed to be negligible for Rb and Cs.

For K, Rb, and Cs [Fig. 8(c)–8(e)], the quantitative agreement of the dispersion curves with the experiments becomes poorer in the low- $q$  region as well as the high- $q$  region. It is mainly due to the small-step diffusion approximation which corresponds to the weak-coupling limit of electron-ion coupling. The small-step diffusion is a realistic representation of atomic motion within RPA which is exact in the limit of high electron density ( $r_s \ll 1$ ).<sup>39</sup> It is asserted that the RPA works reasonably well in Na with  $r_s = 3.9$ , a value which is already beyond the limit of the RPA. Even in potassium with  $r_s = 4.8$ , the RPA gives sensible results.<sup>40</sup> The RPA can be modified by including the exchange and correlation effects with a so-called local-field correction  $G(q)$ . The local field correction given by IU, which is used in the present calculations, is shown to improve the calculation of dynamic structure factor for Li and Na.<sup>41</sup> In light of this, a decent agree-

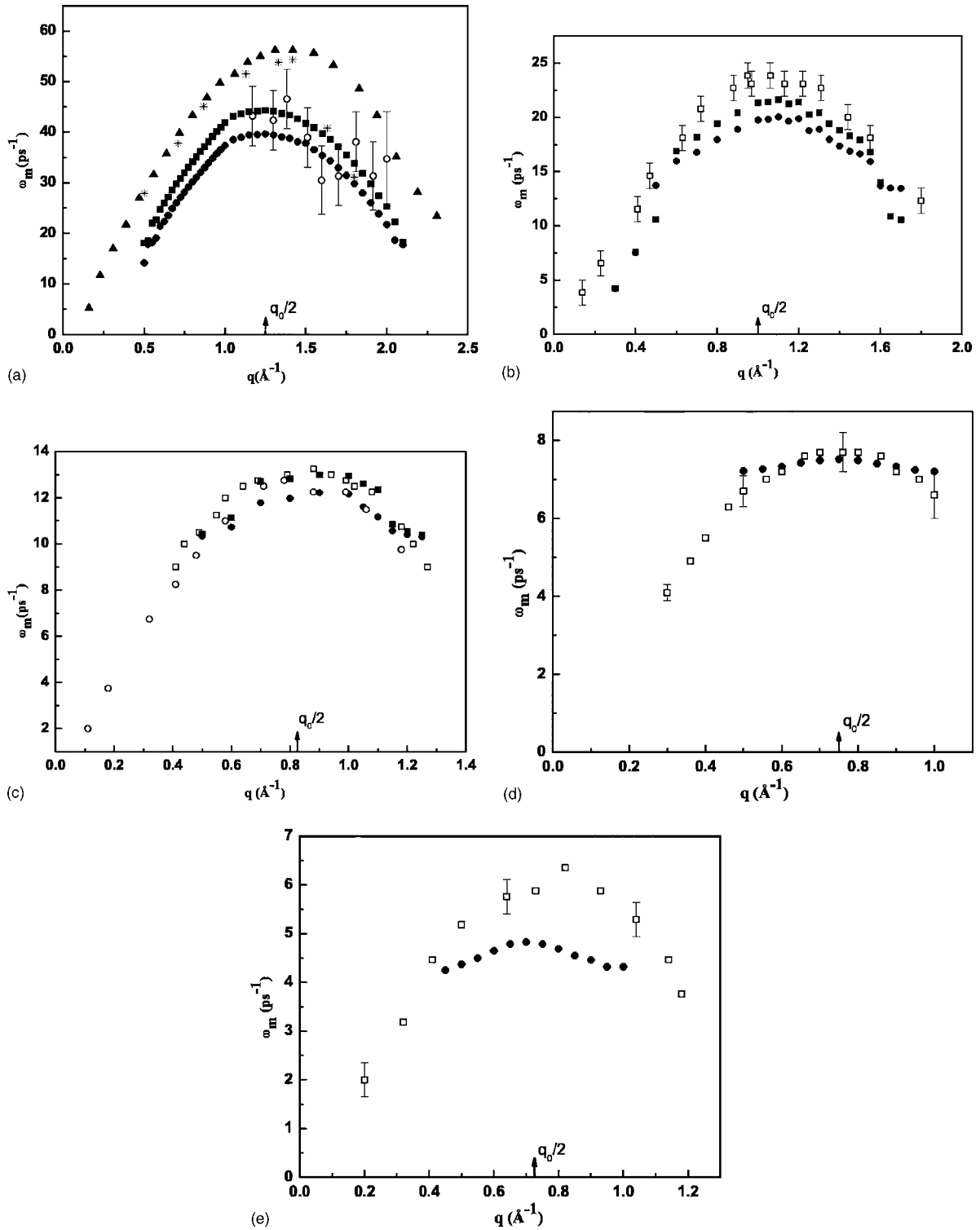


FIG. 8. (a) Dispersion curve for liquid Li. Present results at 463 K (---), Present results at 463 K with the inclusion of quantum-mechanical corrections (■ ■ ■), INS results at 470 K, de Jong *et al.* (Ref. 46) (○ ○ ○), IXS results at 475 K, Scopigno *et al.* (Ref. 47) (▲ ▲ ▲), molecular dynamics results, A. Torcini *et al.* (Ref. 48) (\*\*\*) (b) Dispersion curve for liquid Na. Present results at 378 K (---), present results at 378 K with the inclusion of quantum-mechanical corrections (■ ■ ■), IXS results at 388 K, Pilgrim *et al.* (Ref. 49) (□ □ □). (c) Dispersion curve for liquid K. Present results at 343 K (---), present results at 343 K with the inclusion of quantum-mechanical corrections (■ ■ ■), IXS results at 343 K, Monaco *et al.* (Ref. 50) (○ ○ ○), INS results at 343 K, C. Cabrillo *et al.* (Ref. 2) (□ □ □). (d) Dispersion curve for liquid Rb. Present results at 313 K (---) INS results at 320 K, Copley and Rowe (Ref. 44) (□ □ □). (e) Dispersion curve for liquid Cs. Present results at 303 K (---) and INS results at 308 K, Bodensteiner *et al.* (Ref. 51) (□ □ □).



TABLE IV. Coulomb coupling constant  $r_s$  for liquid alkali metals at melting point;  $\hbar\omega_0$  obtained from Einstein frequency ( $\omega_0$ ) (Table II) and  $V_{\min}(r)$  obtained from the minimum of effective pair potential (Fig. 2).

Metal	$\rho$ ( $\text{\AA}^{-3}$ )	$r_s$	$\hbar\omega_0$ (meV)	$V_{\min}(r)$ (meV)
Li	0.0444	3.3117	28.2	13.4
Na	0.0242	4.0529	10.6	12.9
K	0.0128	5.0116	6.2	12.7
Rb	0.0104	5.3706	3.7	10.4
Cs	0.0083	5.7829	2.8	8.9

ment of our results for Li and Na with the experimental results suggests that the small-step diffusion is valid for the description of collective excitations at electron densities corresponding to  $r_s < 4$ . At  $r_s \cong 4$ , an abrupt change in the dynamical correlation effects due the electron gas is reported to occur.<sup>40</sup> At the same time, it should be noted that the IU local-field correction does not account for the frequency-dependent effects and the resulting dielectric function is considered to be less accurate in describing the dynamic properties such as the detailed features in the spectral function of the density-fluctuation excitations.<sup>15</sup> Thus, the static local-field correction is not sufficient and it would then be logical to include a dynamic local-field correction  $G(q, \omega)$  to improve the results further. Inclusion of  $G(q, \omega)$  is indeed suggested to improve results for Li and Na.<sup>41</sup>

Apart from the limitation imposed by the SSDA, the quantitative discrepancies for Na, K, Rb, and Cs could also be due to the possible failure of GA in the intermediate  $q$  range (Sec. III). The GA holds exactly (in a highly simplified form) in the well-known impulsive regime [governed by the impulse approximation<sup>42</sup> (IA)], where  $\hbar\omega$  becomes much larger than the typical scale of interparticle binding energies.<sup>29</sup> Considering the interparticle binding energy to be the minimum of the interatomic pair potential,  $V_{\min}(r)$  (Fig. 2) and taking Einstein frequency ( $\omega_0$ ) calculated using the average interatomic potential energy  $\langle \nabla^2 V \rangle$  (Table II); the values  $\hbar\omega_0$  and  $V_{\min}(r)$  are given in Table IV. Therefore, it could be suggested that (i) the GA holds well for Li within the impulsive regime [ $\hbar\omega \gg V_{\min}(r)$ ] and (ii) the departure from the impulsive regime on account of increasing importance of interparticle binding energy over  $\hbar\omega_0$  leads to the failure of GA and hence the deterioration in the quantitative agreement of the results for Na, K, Rb, and Cs.

Despite the limitations of SSDA and GA, our results (in general) show a reasonable agreement with experiments in the vicinity of wave vector ( $q_0/2$ ). A significant deviation from the experimental results is observed for Rb and Cs at 0.5 and 0.45  $\text{\AA}^{-1}$ , respectively. Because of the simplicity of the formulation used in this work, it is quite difficult to explain the results for Rb and Cs. However, the observed agreement for Rb can be attributed to the fortuitous balance between the GA and the effect due to strong electron-ion coupling. The balance might deteriorate in the heavier system composed by Cs atoms. Another point that is of more interest to us is the reported anomalous behavior in the dis-

persion curves for Rb and Cs near 0.4  $\text{\AA}^{-1}$ .<sup>43</sup> It has been suggested due to the existence of short-wavelength high-frequency collective modes called “zero-sound-like” modes propagating via an effective interaction potential between the particles as in solids.<sup>43,44</sup> The increased importance of effective interaction potential in Rb and Cs is yet another indication of strong electron-ion coupling where the linear trajectory approximation is more adequate than the SSDA. The strong electron-ion coupling and the softer repulsive core of the interaction potential (Fig. 2) increases the cohesivity of the nearest-neighbor cage which, in turn, implies longer residence time for the diffusing atom inside the cage. In other words, the single-particle dynamics dominates for a longer time and subsequently the density fluctuations persisting for a long time may give rise to propagating short-wavelength collective excitations. The increased cohesivity of the nearest-neighbor cage also favors the formation of small clusters at the length and time scales of present interest. Findings by Morkel *et al.*<sup>43</sup> give some evidence for the existence of small clusters of about 15  $\text{\AA}$  size, as this length scale is resolved around 0.4  $\text{\AA}^{-1}$ . Such a volume contains about 12 to 15 atoms in liquid cesium. From the study of microscopic mechanism of atomic motion in simple liquids by Endo and Endo,<sup>45</sup> the shape of the VACFs in the present investigations (Fig. 5) suggests the number of nearest-neighbor atoms to be equal to 12–14. Thus, according to Morkel *et al.*,<sup>43</sup> for a short time there seems an ensemble of about 15 highly correlated particles to be formed, which shows shear relaxation on the picosecond scale.

## V. CONCLUSIONS

Present work is a sequel of paper I where the single-particle Brownian motion in simple monatomic liquids has been described with the help of the equation of motion in terms of VACF,  $\psi(t)$  [ Eq. (1)], assuming an atom moving in a mean-time-dependent field. In paper I, a generalized solution to the equation of motion has been provided in terms of  $n$ th order Bessel functions of first and second kind. The application of the generalized solution for  $n=2$  (that is  $\beta=3\alpha$ ) to the liquid alkali metals Li and Na was found to give a good description of single-particle motion in terms of VACF. The universal properties exhibited by the liquid alkali metals motivated us to assume that the generalized solution for  $n=2$  [Eq. (10)] could be utilized to study the dynamics of the atomic motion in liquid alkali metals. In addition to the assumption  $n=2$ , employing the small-step diffusion approximation, we could obtain the VACFs for the liquid alkali metals at their melting point. The results evidentially suggest that the repulsive part of the interatomic potential plays a significant role in the atomic motion on the short time scale ( $10^{-12}$  s) and that it bears its signature on the dynamical properties of the liquid alkali metals. The diffusion coefficients, calculated subsequently using VACFs, are in very good agreement with the experimental results. The values of  $D$  calculated from the linear part of the mean-square displacement are also very close to the experimental results. Thus present formulation, along with the aforementioned assumptions, can be conveniently used to study the single-

particle motion in liquid alkali metals. Apart from this, it also provides a reasonable account of the collective motion of the atoms due to the propagation of density fluctuations. The dispersion curves for Li, Na, and K exhibit a decent overall agreement with the experiments and the inclusion of the quantum-mechanical corrections gives a striking improvement in the dispersion curve. For the lower atomic densities (and hence lower electron densities) of Rb and Cs, the formulation seems to be inadequate to represent the collective motion in the low- $q$  (below  $\sim 0.5 \text{ \AA}^{-1}$ ) as well as high- $q$  region (above  $0.9 \text{ \AA}^{-1}$ ). The inadequacy mainly stems from (i) the limitation of SSDA which is valid in the weak electron-ion coupling limit and (ii) the failure of GA beyond impulsive regime. Though, SSDA is reasonable in the RPA limit (high electron densities,  $r_s \ll 1$ ), where XC effect due to electron-ion coupling is excluded, inclusion of XC effects in terms of the so-called IU local-field correction could still give sensible results at lower electron densities (up to  $r_s \sim 5$ ). We remark that (i) relaxing SSDA may improve present formulation to give better description of the dynamical prop-

erties in liquid alkali metals and (ii) our conclusion regarding the failure of GA is rather explorative and not definitive. Finally, an important observation which could be made from the results of the present investigations is that the trend in the dynamical properties of the liquid alkali metals is in accordance to the trend in their atomic number density. An abrupt change in the trend occurs close to potassium position and hence it is considered to possess a key role in drawing a comprehensive view of the properties of the liquid alkali metals.

#### ACKNOWLEDGMENTS

The authors are grateful to Professor J.-F. Wax, Laboratoire de Théorie de la Matière Condensée, Université de Metz, France for his kind help in debugging the program to calculate effective pair potentials. The authors acknowledge the financial assistance by the University Grants Commission, New Delhi under R & D Project No. F10-24/98 (SRI).

\*Email address: kiritlad@yahoo.com

- <sup>1</sup>U. Balucani and M. Zoppi, *Dynamics of the Liquid State* (Clarendon Press, Oxford, 1994).
- <sup>2</sup>C. Cabrillo, F. J. Bermejo, M. Alvarez, P. Verkerk, A. Maria-Vidal, S. M. Bermington, and D. Martin, Phys. Rev. Lett. **89**, 075508 (2002).
- <sup>3</sup>T. Scopigno, G. Ruocco, F. Sette, and G. Vilianni, Phys. Rev. E **66**, 031205 (2002).
- <sup>4</sup>A. V. Mokshin, R. M. Yulmetyev, and P. Hänggi, J. Chem. Phys. **121**, 7341 (2004).
- <sup>5</sup>P. Polanowski and T. Pakula, J. Chem. Phys. **118**, 11139 (2003).
- <sup>6</sup>L. Glass and S. A. Rice, Phys. Rev. **176**, 239 (1968).
- <sup>7</sup>K. N. Lad and A. Pratap, Phys. Rev. E **70**, 051201 (2004).
- <sup>8</sup>U. Balucani, A. Torcini, and R. Vallauri, Phys. Rev. A **46**, 2159 (1992); Phys. Rev. B **47**, 3011 (1993).
- <sup>9</sup>J.-F. Wax, R. Albaki, and J.-L. Bretonnet, J. Non-Cryst. Solids **312-314**, 187 (2002).
- <sup>10</sup>S. A. Rice and J. G. Kirkwood, J. Chem. Phys. **31**, 901 (1959).
- <sup>11</sup>S. Kambayashi and Y. Hiwatari, Phys. Rev. E **49**, 1251 (1994).
- <sup>12</sup>C. Fiolhais, J. P. Perdew, S. Q. Armster, J. M. MacLaren, and M. Brajczewska, Phys. Rev. B **51**, 14001 (1995); **53**, 13193 (1996).
- <sup>13</sup>S. Dalgic, M. Colakogullari, and S. S. Dalgic, J. Optoelectron. Adv. Mater. **7**, 1993 (2005).
- <sup>14</sup>M. Boulahbak, N. Jaske, J.-F. Wax, and J.-L. Bretonnet, J. Chem. Phys. **108**, 2111 (1998); J.-F. Wax, R. Albaki, and J.-L. Bretonnet, Phys. Rev. B **65**, 014301 (2001).
- <sup>15</sup>S. Ichimaru and K. Utsumi, Phys. Rev. B **24**, 7385 (1981).
- <sup>16</sup>H. Mori, Prog. Theor. Phys. **33**, 423 (1965); R. Kubo, Rep. Prog. Phys. **29**, 255 (1966).
- <sup>17</sup>B. J. Berne, J. P. Boon, and S. A. Rice, J. Chem. Phys. **45**, 1086 (1966).
- <sup>18</sup>U. Balucani, A. Torcini, A. Stangl, and C. Morkel, Phys. Scr. **T57**, 13 (1995).
- <sup>19</sup>G. E. Uhlenbeck and L. S. Ornstein, Phys. Rev. **36**, 823 (1930).
- <sup>20</sup>The term  $\omega_0^2 e^{-at}$  appearing in Eq. (25) of paper I is a typographical mistake. In stead of  $\omega_0^2 e^{-at}$ , it should be  $\omega_0^2$  only.

- <sup>21</sup>V. F. Sears, Proc. Phys. Soc. London **86**, 953 (1965).
- <sup>22</sup>R. A. Harris and S. A. Rice, J. Chem. Phys. **33**, 1055 (1960).
- <sup>23</sup>R. C. Desai and S. Yip, Phys. Rev. **166**, 129 (1968); **180**, 299 (1969).
- <sup>24</sup>G. H. Vineyard, Phys. Rev. **110**, 999 (1958).
- <sup>25</sup>K. Sköld, Phys. Rev. Lett. **19**, 1023 (1967).
- <sup>26</sup>P. G. De Gennes, Physica (Amsterdam) **25**, 825 (1959).
- <sup>27</sup>G. Venkataraman, B. A. Dasannacharya, and K. R. Rao, Phys. Rev. **161**, 133 (1967).
- <sup>28</sup>A. Rahman, K. S. Singwi, and A. Sjölander, Phys. Rev. **126**, 986 (1962).
- <sup>29</sup>D. Colognesi, M. Celli, M. Neumann, and M. Zoppi, Phys. Rev. E **70**, 061202 (2004).
- <sup>30</sup>T. Tsang, Phys. Rev. A **17**, 393 (1978).
- <sup>31</sup>L. E. Gonzalez, D. J. Gonzalez, and M. Canales, Z. Phys. B: Condens. Matter **100**, 601 (1996).
- <sup>32</sup>L. F. Bove, B. Dorner, C. Paetrillo, F. Sacchelti, and J.-B. Suck, Phys. Rev. B **68**, 024208 (2003).
- <sup>33</sup>D. P. Dean and J. N. Kushick, J. Chem. Phys. **76**, 619 (1982).
- <sup>34</sup>T. Gaskell and P. E. Mason, J. Phys. C **14**, 561 (1981).
- <sup>35</sup>S. D. Wijeyesekera and J. N. Kushick, J. Chem. Phys. **71**, 1397 (1979).
- <sup>36</sup>J. Kushick and B. J. Berne, J. Chem. Phys. **59**, 3732 (1973).
- <sup>37</sup>T. Scopigno, U. Balucani, G. Ruocco, and F. Sette, J. Phys.: Condens. Matter **12**, 8009 (2000).
- <sup>38</sup>T. Scopigno, G. Ruocco, and F. Sette, Rev. Mod. Phys. **77**, 881 (2005).
- <sup>39</sup>S. A. Rice, G. Nicolis, and J. Jortner, J. Chem. Phys. **48**, 2484 (1968).
- <sup>40</sup>G. Kalman, K. Kempa, and M. Minella, Phys. Rev. B **43**, 14 238 (1991).
- <sup>41</sup>J. P. Hill, C.-C. Kao, W. A. C. Caliebe, D. Gibbs, and J. B. Hastings, Phys. Rev. Lett. **77**, 3665 (1996).
- <sup>42</sup>S. W. Lovesey, *Theory of Neutron Scattering from Condensed Matter* (Oxford University Press, Oxford, 1987), Vol. I.

- <sup>43</sup>Chr. Morkel, T. Bodensteiner, and H. Gemperlein, Phys. Rev. E **47**, 2575 (1993).
- <sup>44</sup>J. R. D. Copley and J. M. Rowe, Phys. Rev. Lett. **32**, 49 (1974).
- <sup>45</sup>Y. Endo and H. Endo, Phys. Lett. **95A**, 92 (1983).
- <sup>46</sup>P. H. K. de Jong, P. Verkerk, and L. A. de Graff, J. Non-Cryst. Solids **156-158**, 48 (1993).
- <sup>47</sup>T. Scopigno, U. Balucani, A. Cunsolo, C. Masciovecchio, G. Ruocco, and F. Sette, Philos. Mag. B **79**, 2027 (1999).
- <sup>48</sup>A. Torcini, U. Balucani, P. H. K. de Jong, and P. Verkerk, Phys. Rev. E **51**, 3126 (1995).
- <sup>49</sup>W.-C. Pilgrim, S. Hosagawa, H. Saggan, H. Sinn, and E. Burkel, J. Non-Cryst. Solids **250-252**, 96 (1999).
- <sup>50</sup>A. Monaco, T. Scopigno, P. Benani, A. Giugni, G. Monaco, M. Nardone, G. Ruocco, and M. Sampoli, J. Chem. Phys. **120**, 8089 (2004).
- <sup>51</sup>T. Bodensteiner, Chr. Morkel, and W. Glaser, Phys. Rev. A **45**, 5709 (1992).